Heliyon 10 (2024) e34509

Contents lists available at ScienceDirect

Heliyon

journal homepage: www.cell.com/heliyon

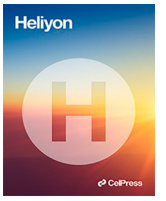

Research article

G protein-coupled receptor 91 promotes the inflammatory response to *Porphyromonas gingivalis* in bone marrow-derived macrophages

Wenqi Su [a,c], Yujia Wang [a,c], Cancan Zu [a,c], Lang Lei [b], Houxuan Li [a,*]

[a] *Department of Periodontics, Nanjing Stomatological Hospital, Affiliated Hospital of Medical School, Institute of Stomatology, Nanjing University, Nanjing, China*
[b] *Department of Orthodontics, Nanjing Stomatological Hospital, Affiliated Hospital of Medical School, Institute of Stomatology, Nanjing University, Nanjing, China*
[c] *Central Laboratory of Stomatology, Nanjing Stomatological Hospital, Affiliated Hospital of Medical School, Institute of Stomatology, Nanjing University, Nanjing, China*

ARTICLE INFO

Keywords:
GPR91
P. gingivalis
Bone marrow-derived macrophages
Periodontitis
Succinate
Nuclear factor-κB

ABSTRACT

Macrophages are important for maintaining tissue homeostasis and defending against pathogens in periodontal tissues. However, these tissues are often vulnerable to damage due to local inflammatory responses within the host tissues. This study aimed to investigate the role of G protein-coupled receptor 91(GPR91) during the inflammatory response to *Porphyromonas gingivalis* (*P. gingivalis*) in bone marrow-derived macrophages (BMDMs). To this end, we examined expression levels of GPR91 genes in human periodontal tissues affected by periodontitis. Utilizing primary mouse BMDMs from wild-type (WT) and GPR91 knockout ($GPR91^{-/-}$) mice infected with *P. gingivalis*, we demonstrated that GPR91 accumulates in inflamed gingival tissues. Additionally, *P. gingivalis* can induce intercellular succinate accumulation, inflammatory mediator generation, reactive oxygen species (ROS) production, lipid peroxidation, and superoxide dismutase activity in WT-BMDMs. Moreover, inhibition of GPR91 by the specific inhibitor 4C as well as knockdown of GPR91 reduced inflammation and oxidative stress in *P. gingivalis*-infected BMDMs. Furthermore, we discovered that GPR91-mediated inflammation in *P. gingivalis*-infected BMDMs is activated via the Erk/Nuclear Factor-κB pathway. These findings provide new insights into the metabolic pathogenesis of periodontal inflammation.

1. Introduction

Periodontitis is a chronic inflammatory disease that affects all parts of the periodontium, potentially leading to irreversible damage within the periodontal microenvironment. *Porphyromonas gingivalis* (*P. gingivalis*), a gram-negative oral anaerobe, plays an important role in the pathogenesis of periodontitis [1]. Including excessive production of gingipain proteinases, outer membrane vesicles, and lipopolysaccharides, *P. gingivalis* triggers an inflammatory cascade characterized by immune cell infiltration of macrophages and neutrophils, among other components [2]. Such bacterial invasions result in the activation of inflammatory cells that release various inflammatory mediators as part of the host's defense response [3].

* Corresponding author.
E-mail address: lihouxuan3435_0@163.com (H. Li).

https://doi.org/10.1016/j.heliyon.2024.e34509
Received 18 January 2024; Received in revised form 5 July 2024; Accepted 10 July 2024
Available online 14 July 2024

The inflammatory responses to bacterial stimuli in defense cells are characterized by changes in the energy production system, shifting from slow but highly efficient oxidative phosphorylation to quick but less efficient glycolysis [4]. Similarly, *P. gingivalis* infection increases glycolysis in osteoblasts and promotes the production of the receptor activator of NF-κB (RANK) ligand (RANKL), increasing elevated osteoclastogenesis and alveolar bone resorption in the periodontal niche [5]. In addition, *P. gingivalis* infection disrupts the tricarboxylic acid cycle, leading to the accumulation of succinate in the mitochondria and cytoplasm of periodontal ligament fibroblasts [6].

Once succinate accumulates in the cytosol, it can enter the extracellular environment, although the process by which is does so has not yet been identified. Succinate is a natural ligand for G protein-coupled receptor 91 (GPR91), which is located on the cell membrane [7]. G protein-coupled receptors (GPRs) are widely distributed on the cell membrane and detect changes in the cellular environment. Thus, their activation plays an important role in transmembrane signaling pathways that recognize and transmit extracellular stimuli into cells[8]. Activation of GPR91 may trigger a cascade of the downstream signaling pathway, including the phospholipase C (PLC)-IP3, diacylglycerol (DAG), and adenylyl cyclase (AC)-cAMP pathway [9].

Importantly, the GPR91 signaling axis plays a complex role in the immunity and inflammation responses [10]. Dendritic cells (DCs) sense succinate via GPR91, stimulating antigen presenting cells to enhance immunity [11]. Other research has shown that in vitro stimulation of macrophages with interleukin (IL)-4 can increase GPR91 expression [12]. However, succinate or GPR91 activator stimulation decreases the expression of the anti-inflammatory cytokine IL-10 while upregulating the pro-inflammatory cytokine tumor necrosis factor-α (TNF-α), thereby improving the pro-inflammatory response [7]. Taken together, these activities suggest that the effects of GPR91 vary in different disease conditions.

Several studies have linked extracellular succinate-activated GPR91 to various diseases, including pathological cardiomyocyte hypertrophy [13], rheumatoid arthritis [14], and the pathogenesis of diabetic nephropathy [15]. However, the role of GPR91 in regulating macrophage defense during bacterial infection remains to be relatively unknown. In this study, we investigated the cellular processes after GPR91 activation in response to *P. gingivalis* infection in macrophages, and our present study provided new insights into the metabolic pathogenesis of periodontal diseases.

2. Materials and methods

2.1. Clinical Specimens

The Medical Ethics Committee of Nanjing Stomatological Hospital, Medical School of Nanjing University approved this study (2018NL-007(KS)). Normal gingival tissues (n = 10) and inflamed gingival tissues (n = 10) were obtained after informed consent of the patients as we described previously [16]. Patients with histories of systematic diseases were excluded in the study. For the healthy group, gingival tissues were harvested during crown lengthening surgery, wisdom tooth extraction or gingivectomy upon exposure of impacted teeth during orthodontic treatment. All the sampling sites displayed no gingival redness and swelling, was negative bleeding after probing with probing depth of less than 3 mm and no attachment loss. The inflammatory gingival tissues were obtained from hopeless teeth with degree III mobility, and the patients received no periodontal treatment and had no medical history of taking immunosuppressive agents and anagentstics in the last 6 months.

2.2. Mice and cell culture

Ethical Review Committee for Experimental Animal Welfare, Nanjing University (IACUC-D2202111) approved the study protocol. C57BL/6 mice and GPR91 knockout mice ($GPR91^{-/-}$) of 6–8 weeks of age were generated and identified by GemPharmatech (GemPharmatech Co. Ltd., Nanjing, China). The mice were bred in a specific-pathogen free (SPF) sterile environment with a temperature of 22 °C, relative humidity of 60 %, and daily light duration of 12 h. Mice were sacrificed by cervical dislocation and sterilized with 75 % ethanol for 15 min. Then the femurs and tibiae were collected and ice-cold PBS flushed out the bone marrow cells in the medullary cavity. Supernatants were collected in ice-cold PBS and filtered through a 70 μm nylon cell strainer to remove solid fragments. The filtrate was centrifuged at 1000 rounds per min for 5 min at 4 °C, and red blood cell lysis buffer (Beyotime, China) removed the erythrocytes. The bone marrow cells were differentiated into murine bone marrow-derived macrophages (BMDMs) as previously described [17] by using 1640 conditioned medium for 7 days. The culture medium was composed of RPMI 1640 medium (Gibco, USA) with 10 % fetal bovine serum (FBS) (Gibco, Australia), 1 % penicillin/streptomycin solution, and 30 % L929 conditioned medium.

2.3. Bacterial strains

P.gingivalis strain (ATCC 33277) was grown anaerobically in a modified BHI medium (contains 5 mg/ml hemin, 1 mg/ml menadione,and 1 mg/ml yeast extract) at 37 °C with 85 % N_2, 5 % H_2, and 10 % CO_2 overnight to obtain live bacteria in the exponential growth. Using a spectrophotometer, the bacterial concentrations were standardized to an optical sdensity of 1 at 600 nm, which corresponds to 1×10^9 CFU/ml. BMDMs were seeded in 2×10^6/6-well plate, 8×10^3/96-well plate, and 8×10^5/35 mm confocal dishe. The BMDMs were infected with *P. gingivalis* (multiplicity of infection = 10, 50, 250) and its infection time varied in different experiments and was described in the figure legends, respectively. The GPR91-antagonist 4C was synthesized by Wuhe BioTech Co., China, and 4C (5 μM, the final concentration in the cell culture) was added to the culture medium 2 h before bacterial stimulation.

2.4. Immunohistochemistry

The gingival tissue samples were soaked in 4 % paraformaldehyde for 24 h and fixed with wax. Then, the tissue was cut into 3 μm thickness and incubated with anti-GPR91(1:200, Biorbyt, orb157370) at 4 °C overnight after the regular chemical processes and followed by incubation of secondary antibodies (MaxVision, KIT-5010, China) at 37 °C for 30 min. The IHC scores were determined as described previously [18] under the chromogenic Diaminobenzidine (DAKO, USA) was used as a chromogenic agent to detect antibody binding. The percentage of positive cells in ten random visual fields for healthy and periodontitis tissues, was counted with Image-J software (V1.8.0, National Institutes of Health, USA) by two independent observers who were blinded to the samples, respectively.

2.5. ROS and iNOS detection by flow cytometry and immunofluorescence

Intracellular reactive oxygen species (ROS) in BMDMs were detected using the reactive oxygen species assay kit (S0033S, Beyotime, China). BMDMs differentiated from the bone marrow cells were seeded at a density of 1×10^6 cells in a 6-well cell culture plate and treated with *P.gingivalis* for 24 h. Cells were incubated with 10 μM DCFH-DA reagent for 30 min at 37 °C and stained with an anti-mouse inducible nitric oxide synthase (iNOS) antibody (1:250, CST, D6B6S). The color reactions of images were captured on confocal microscopy (Nikon A1, Japan). Subsequently, cells were scraped in the PBS, before being transferred to the polypropylene FACS tubes. The stained cells were analyzed with FlowJo software (Tree Star, USA) and data were analyzed with FlowJo v.9.5.2 software (Tree Star).

2.6. Quantitative PCR

Gingival tissues were ground with lysate, centrifuged at 12000 rpm/min for 10 min. The supernatant after centrifugation was taken and the subsequent RNA extraction process was carried out according to the reagent instructions. After washing the BMDMs in the 6-well plate with PBS for 3 times, the lysate was added, thoroughly mixed, and the RNA was extracted after the liquid was collected. Total gingival mRNA and the total RNA from BMDMs were extracted by total RNA extraction reagent (Vazyme, China). In the 10 μl reverse transcription system, 2 μl 5X Evo M-MLV RT Master Mix was added. According to the concentration of extracted RNA, the volume of added RNA was calculated with the total RNA of 500 ng, and 10 μl was supplemented with ddH_2O. The whole process was carried out on ice. The reverse transcription of RNA used the cDNA synthesis kit (Accurate biology, China). The sequences of the primers for quantitative real-time PCR (qPCR) were inquired by PrimerBank and synthesized by Genscript (Genscript, China). The sequences of primers were present in Table 1. The relative quantification was calculated by the method of comparative $2^{-\Delta\Delta Ct}$.

2.7. Western blot

Gingival tissues were immediately stored at −80 °C after excision. The tissues were cut into pieces, lysed with the RIPA lysis buffer (Beyotime, China), and homogenized with a homogenizer. BMDMs were lysed with the RIPA. The protein concentration was determined via a Nanodrop (Thermo Fisher Scientific, USA). According to the total protein amount of 30 ng/ml in each lane, and proteins were separated by 4–20 % SDS-PAGE (Smart-Lifesciences, China) at a voltage of 160 V for 40 min, transferred to the PVDF membrane (Millipore,USA), and blocked with Quick Block™ blocking buffer (Beyotime, China). The membrane was blocked with 5 % bovine albumin and then incubated with primary antibodies: rabbit anti-β-actin (1:1000; 66009-*l*-lg, Proteintech, China), rabbit anti-GPR91 (1:1000, Biorbyt, orb157370), rabbit anti-IL-1β (1:1000, CST, 12242s), rabbit anti-IL-6 (1:1000, Proteintech, 21865-I-AP), rabbit anti-TNFα (1:1000, Servicebio, GB11188), rabbit anti-iNOS (1:1000, CST, D6B6S), rabbit anti-P65 (1:1000, CST, D14E12), rabbit anti-p-P65 (1:1000, CST, 93H1), rabbit anti-Erk (1:1000, Servicebio, GB11560), rabbit anti-*p*-Erk (1:1000, Affinity, AF1015), and secondary antibodies (1:1000, Thermo Fisher Scientific, USA). Image Quant LAS 4000 was used to detecte the result of color reactions. Western blot was performed three times independently.

2.8. Enzyme-linked immunosorbent assay

BMDMs cells were treated with *P. gingivalis* for 24 h. The levels of mouse IL-1β (LA128804H, Lapuda, China)、IL-6 (LA128802H, Lapuda, China) and TNF-α (LA128801H, Lapuda, China) in culture supernatants were detected by the inflammatory cytokines assay

Table 1
The primer sequences used for real-time qPCR.

Genes	Sequence(5′-3′)	Sequence(3′-5′)	PrimerBank ID
IL-1β (mouse)	GCAACTGTTCCTGAACTCAACT	ATCTTTTGGGGTCCGTCAACT	6680415a1
IL-6 (mouse)	TAGTCCTTCCTACCCCAATTTCC	TTGGTCCTTAGCCACTCCTTC	13624311a1
TNFα (mouse)	CCCTCACACTCAGATCATCTTCT	GCTACGACGTGGGCTACAG	7305585a1
iNOS (mouse)	GTTCTCAGCCCAACAATACAAGA	GTTCTCAGCCCAACAATACAAGA	6754872a1
GPR91 (mouse)	TCTTGTGAGAATTGGTTGGCAA	CATCTCCATAGGTCCCCTTATCA	14161704a1
β-actin (mouse)	GGCTGTATTCCCCTCCATCG	CCAGTTGGTAACAATGCCATGT	6671509a1
GPR91 (human)	GGAGACC CCAACTACAACCTC	AGCAACCTGCCTATTCCTCTG	260593714c1
β-actin (human)	CATGTACGTTGCTATCCAGGC	CTCCTTAATGTCACGCACGAT	4501885a1

kits, respectively. The culture supernatants were centrifuged at 1500 rpm for 20 min and was collected carefully. The detection was performed following the manufacture's protocol. The optical density of each well was determined immediately using a microplate reader set to 450 nm. The optical density (OD) value of the blank hole was subtracted from the OD value of the sample hole. The standard curve was made according to the concentration and OD of the standard substance. The OD was read by SpectraMax M3 (Molecular Devices, Sunnyvale, CA, USA).

2.9. Nitric oxide detection

BMDMs were treated with *P. gingivalis* for 24 h. NO production in the cell culture medium was measured using a total nitric oxide assay kit (S0021S, Beyotime, China) according to the manufacturer's protocol. Absorbance at 540 nm was measured using SpectraMax M3 (Molecular Devices, Sunnyvale, CA, USA).

2.10. Lipid peroxidation and superoxide dismutase

According to the manufacturer's protocol, malondialdehyde (MDA) (S0131S, Beyotime, China) and total superoxide dismutase (SOD) (S0101S, Beyotime, China) activity were measured using a WST-8-based color reaction. The generation of malondialdehyde (MDA) was used to measure lipid peroxidation. Cells were harvested by trypsinization and cellular extracts were prepared by sonication in ice-cold buffer. After sonication, lysed cells were centrifuged at 10,000g for 10 min to remove debris. The supernatant was subjected to the measurement of MDA levels and total SOD. The protein concentration of each sample was determined by Nanodrop (Thermo Fisher Scientific, USA).

2.11. Immunofluorescence

The BMDMs were seeded onto 35 mm confocal dishes with 8×10^5 cells per well overnight, and *P. gingivalis* was stimulated with MOI = 50 for 12 h. Then washed 3 times with PBS and fixed in 4 % paraformaldehyde for 15 min. Cell and gingival tissue were permeabilized with iced methanol, and blocked with 5 % BSA. Then gingival tissues and cells were incubated with rabbit anti-GPR91 (1:250, Biorbyt, orb157370), rabbit anti-iNOS (1:200, D6B6S, CST), rabbit anti-*p*-Erk (1:400, Affinity, AF1015), and rabbit anti-p-P65 (1:400, CST, 93H1) at 4 °C overnight. Subsequently, gingival tissues were incubated with Cy5 648 goat anti-Rabbit IgG (1:200,

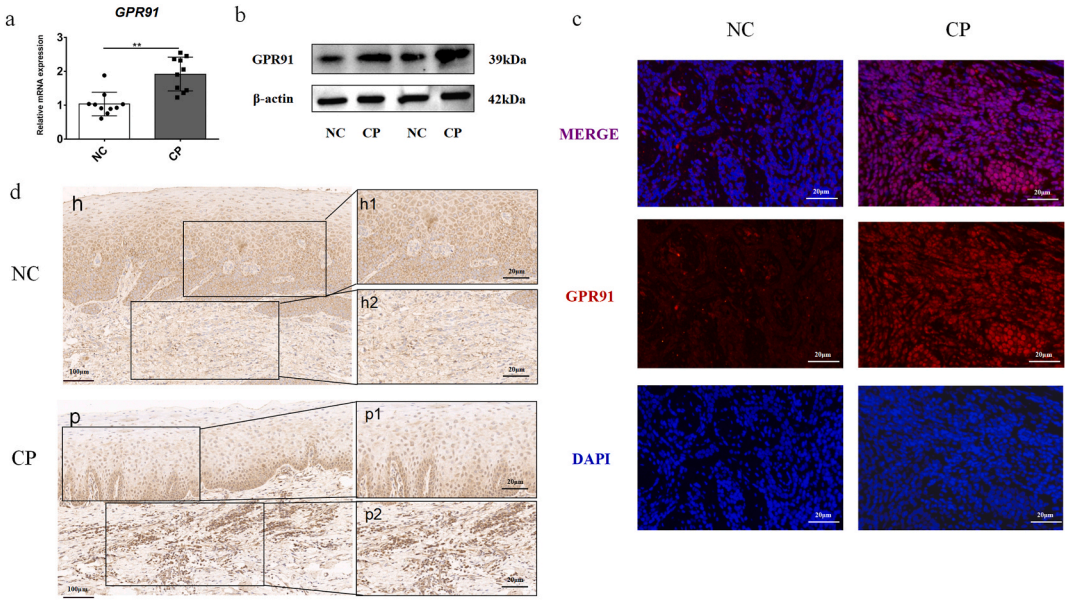

Fig. 1. Increased GPR91 expression in the inflammatory periodontal tissues. (a) Gene transcription level of GPR91 in normal control (NC, n = 10) and gingival tissues with chronic periodontitis (CP, n = 10) as measured by real-time qPCR. (b) Protein expression of GPR91 in the gingival tissue from normal control (n = 2) or chronic periodontitis (n = 2) were evaluated by Western Blot. More details were shown in the Supplemental Information S1. Gingival tissue from normal control (n = 5) and chronic periodontitis (n = 5) were stained by immunofluorescence (c) and immunohistochemistry (d) stainning. In all cases, bars in graphs represent mean ± SEM. The images were collected from different gels with the same number of samples. NC:normal control,CP:chronic periodontitis. The data were analyzed by Student's t-test, and values are presented as the mean ± SD; *, $p < 0.05$; **, $p < 0.01$. Figures h and p represent the expression of GPR91 in the gingival tissue of the normal control group and chronic periodontitis group at low magnification, respectively. Figures h1/2 represent the expression of GPR91 in the epithelial and connective tissue of the normal control group at higher magnification. Figures p1-2 represent the expression of GPR91 in the epithelial tissue and connective tissue of the chronic periodontitis group at higher magnifcation.

GB27303, Servicebio), while BMDMs were incubated with Cy3 550 Goat Anti-Rabbit IgG (1:200, GB21303, Servicebio) and Alexa Fluor 488 Goat anti-Rabbit IgG (1:200, GB25303, Servicebio) at room temperature for 1 h. Nuclei were stained with 4′, 6-diamidino-2-phenylindole (DAPI, C1005, Beyotime, China). The color reactions of images were captured on confocal microscopy (Nikon A1, Japan). Immunofluorescence was performed three times independently.

2.12. Date statistical analysis

Data were evaluated by one-way analysis of variance (ANOVA; parametric) or the Kruskal–Wallis test (nonparametric) was performed, followed by Bonferroni's multiple comparisons test. Where appropriate (comparison of two groups only), differences between two groups were evaluated using a two-tailed Student's t-test (parametric) or the Mann-Whitney *U* test (nonparametric). The data was presented by GraphPad Prism 9.00 (GraphPad Software Inc, LaJolla, CA, USA). A value of $p < 0.05$ was considered significantly. All experiments have been repeated independently at least 3 times.

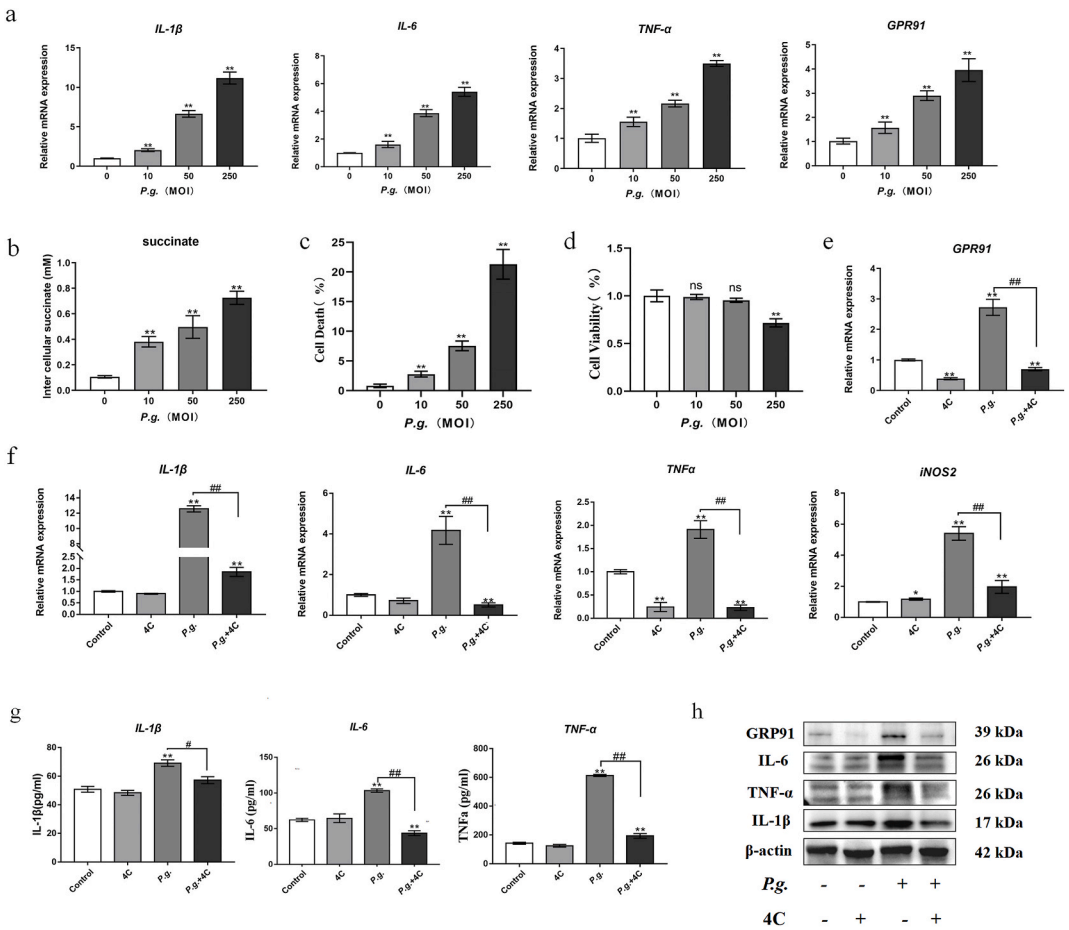

Fig. 2. *P. gingivalis*-induced macrophage inflammation reduced via GPR91 inhibition. BMDMs from WT mice were cultured with different multiplicity of infections (MOIs) of *P. gingivalis*. (a) The expressions of IL-1β, IL-6, TNFα, and GPR91 as detected by real-time qPCR at 4 h. (b) Intercellular succinate concentrations were measured after 24 h of infection. Cells were pretreated with 4C (GPR91 antagonist, 5 μM) for 2 h and infected with *P. gingivalis* (MOI = 50). (c) LDH assay was conducted to measure cell death at 24 h following bacterial infection. (d) Cell Counting Kit-8 (CCK-8) was utilized to detect the cell activity of BMDMs at 24 h. (e&f) Gene transcription level were assessed by real-time qPCR at 4 h. (g) Cytokine expression in the culture supernatants was measured by ELISA at 24 h. (h) Protein levels of protein lysate were analyzed by WesternBlot at 24 h. Image is of a representative Western Blot from one independent experiment. More details were shown in the Supplemental Information S1. Western Blot was performed three times independently. In all cases, bars in graphs represent mean ± SEM. β-actin was adopted as an internal reference. The data were analyzed by ANOVA and a Dunnett multiple-comparison test; *, $p < 0.05$; **, $p < 0.01$ compared with the control; #, $p < 0.05$; ##, $p < 0.01$ compared with the *P. gingivalis*-treated group.

3. Results

3.1. Elevated GPR91 expression levels in the inflamed periodontal tissues

We initially explored whether GPR91 expression was elevated in the gingival tissues of patients with chronic periodontitis. GPR91 transcription was significantly higher in the chronic periodontitis groups compared with healthy controls, as demonstrated by qPCR (Fig. 1a). Similarly, Western blot analysis confirmed elevated GPR91 protein expression levels in the inflamed gingiva (Fig. 1b and Supplemental Information S1). In addition, immunofluorescence analysis showed increased expression levels of GPR91 in inflammatory tissues (Fig. 1c). Furthermore, an examination of GPR91 protein levels in healthy and inflamed tissues via immunohistochemistry revealed more positive staining of GPR91 in the inflamed gingival tissues compared to healthy tissues (Fig. 1d). Collectively, these results indicate that the expression of GPR91 is upregulated in periodontitis.

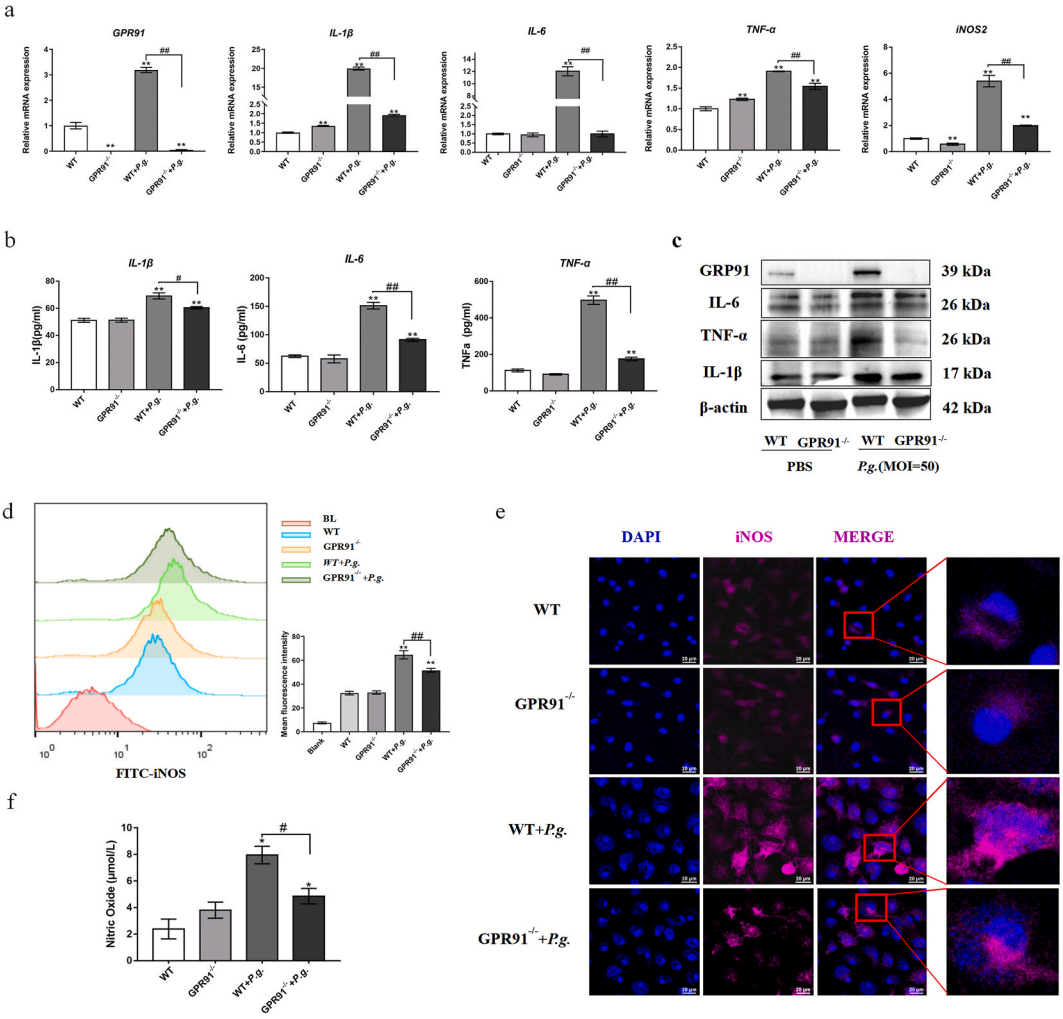

Fig. 3. Effect of GPR91 knockout on inflammatory response during *P. gingivalis* infection in BMDMs.BMDMs from GPR91$^{-/-}$ and WT mice were infected with *P. gingivalis* (MOI = 50). (a) Gene Expression levels were measured by real-time qPCR at 4 h. (b) Cytokine expression in the culture supernatants was measured by ELISA at 24 h. (c) Protein levels were analyzed by Western Blot at 24 h. Image is of a representative Western Blot from one independent experiment. More details were shown in the Supplemental Information S1. (d&e) Inducible nitric oxide synthase (iNOS) was detected by flow cytometry or fluorescence microscope at 18 h. (f) The culture supernatants were collected to measure NO by nitrate reductase assay at 24 h. The scale bar represents 20 μm. Figures e and f represent representative images of an independent experiment in three repeated Western Blot and immunofluorescence experiments. Three regions of each sample extracted in the immunofluorescence assay were photographed. In all cases, bars in graphs represent mean ± SEM. β-actin was adopted as an internal reference. The data were analyzed by ANOVA and a Dunnett multiple-comparison test; *, $p < 0.05$; **, $p < 0.01$ compared with the WT group; #, $p < 0.05$; ##, $p < 0.01$ compared with the WT + *P. g.*-treated group.

3.2. Decreased inflammatory response to P. gingivalis infection in BMDMs following GPR91 inhibition

Macrophages are among the primary immune cells in gingival tissues affected by chronic periodontitis. In this study, bone marrow-derived macrophages (BMDMs) were initially cultured with *P. gingivalis* at multiplicities of infection (MOI) of 10, 50, and 250 for 4 h. The results revealed a gradual upregulation in the expression of proinflammatory cytokines and GPR91 with increasing MOI (Fig. 2a). Additionally, intercellular succinate levels increased with the degree of *P. gingivalis* infection (Fig. 2b). We further investigated whether *P. gingivalis* infection induced cell death in BMDMs and its impact on cell activity. After 24 h, less than 10 percent cell death was observed at an MOI of 50, whereas this value increased to over 20 percent at an MOI of 250 (Fig. 2c). Furthermore, the presence of bacterial infection significantly affected BMDM activity at the MOI of 250 at 24 h, while low-dose bacterial stimulation had no significant effect on cell activity (Fig. 2d).

To further investigate the role of GPR91 in the periodontal inflammatory microenvironment, we pretreated BMDMs with 4C, a specific GPR91 inhibitor, and subsequently infected the BMDMs with *P. gingivalis* at an MOI of 50. It was observed that *P. gingivalis* promoted GPR91 expression, whereas treatment with 4C decreased both the gene transcription and protein expression of GPR91 (Fig. 2e&h and Supplemental Information S1). Inhibition of GPR91 via 4C attenuated the transcriptional levels of pro-inflammatory IL-1β, IL-6, and TNF-α (Fig. 2f); moreover, 4C pretreatment reduced the expression of IL-1β, IL-6, and TNF-α both intracellularly and in the supernatant following *P. gingivalis* infection (Fig. 2g&h and Supplemental Information S1).

3.3. GPR91 knockout dampens inflammatory responses in BMDMs following P. gingivalis infection

To further explore the role of GPR91 activation in the progression of periodontitis, we treated BMDMs from GPR91$^{-/-}$ and WT mice with *P. gingivalis* at the MOI of 50. Transcriptional analysis revealed significantly higher levels of IL-1β, IL-6, TNF-α, iNOS, and GPR91 in WT-BMDMs compared to GPR91$^{-/-}$ BMDMs (Fig. 3a). Similarly, lower levels of IL-1β, IL-6, TNF-α, and GPR91 proteins were detected in GPR91$^{-/-}$ compared to WT-BMDMs (Fig. 3b&c and Supplemental Information S1).

Inducible nitric oxide synthase (iNOS) is a key enzyme involved in the metabolism of reactive oxygen species and nitrogen metabolites. Nitric oxide (NO), derived from iNOS, plays an important role in numerous physiological processes such as blood pressure regulation, wound repair, and host defense, as well as pathophysiological conditions including inflammation, infection, neoplastic diseases, liver cirrhosis, and diabetes [19]. We further analyzed iNOS and NO expression in BMDMs infected with *P. gingivalis,* and the flow cytometry and immunofluorescence results revealed reduced iNOS levels in the *P. gingivalis*-treated BMDMs of GPR91$^{-/-}$ mice compared to WT mice (Fig. 3d–f). Additionally, the generation of NO, the enzymatic synthesis product of iNOS, was diminished in the BMDMs of the GPR91 knockout mice (Fig. 3e).

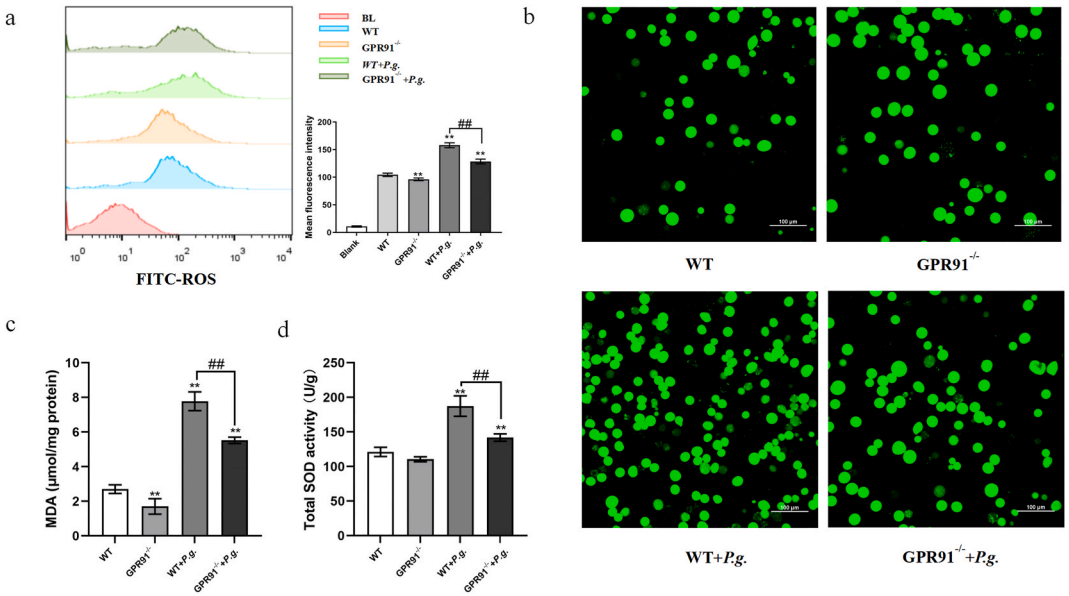

Fig. 4. Reduced oxidative stress in *P. gingivalis*-infected BMDMs via GPR91 knockout. BMDMs from GPR91$^{-/-}$ and WT mice were infected with *P. gingivalis* (MOI = 50). (a&b) Intracellular reactive oxygen species (ROS) were detected by flow cytometry or fluorescence microscope at 12 h. Analysis of MDA (c) production and total SOD (d) in BMDMs after 24 h of *P. gingivalis* infection. The scale bar represents 100 μm. In all cases, bars in graphs represent mean ± SEM. The data were analyzed by ANOVA and a Dunnett multiple-comparison test; *, $p < 0.05$; **, $p < 0.01$ compared with the WT group; #, $p < 0.05$; ##, $p < 0.01$ compared with the WT + *P. g.*-treated group.

3.4. GPR91 knockout reduces ROS production and lipid peroxidation in P. gingivalis -infected BMDMs

Prior studies have identified a link between oxidative stress and inflammation, with evidence suggesting that such stress may also amplify the inflammatory response [20]. The progression of periodontal diseases is often accompanied by excessive generation of reactive oxygen species (ROS) [21]. In this study, we further examined ROS generation in the BMDMs of GPR91 knockout mice following 12 h of *P. gingivalis* infection. Flow cytometry and immunofluorescence analyses revealed that *P. gingivalis* infection

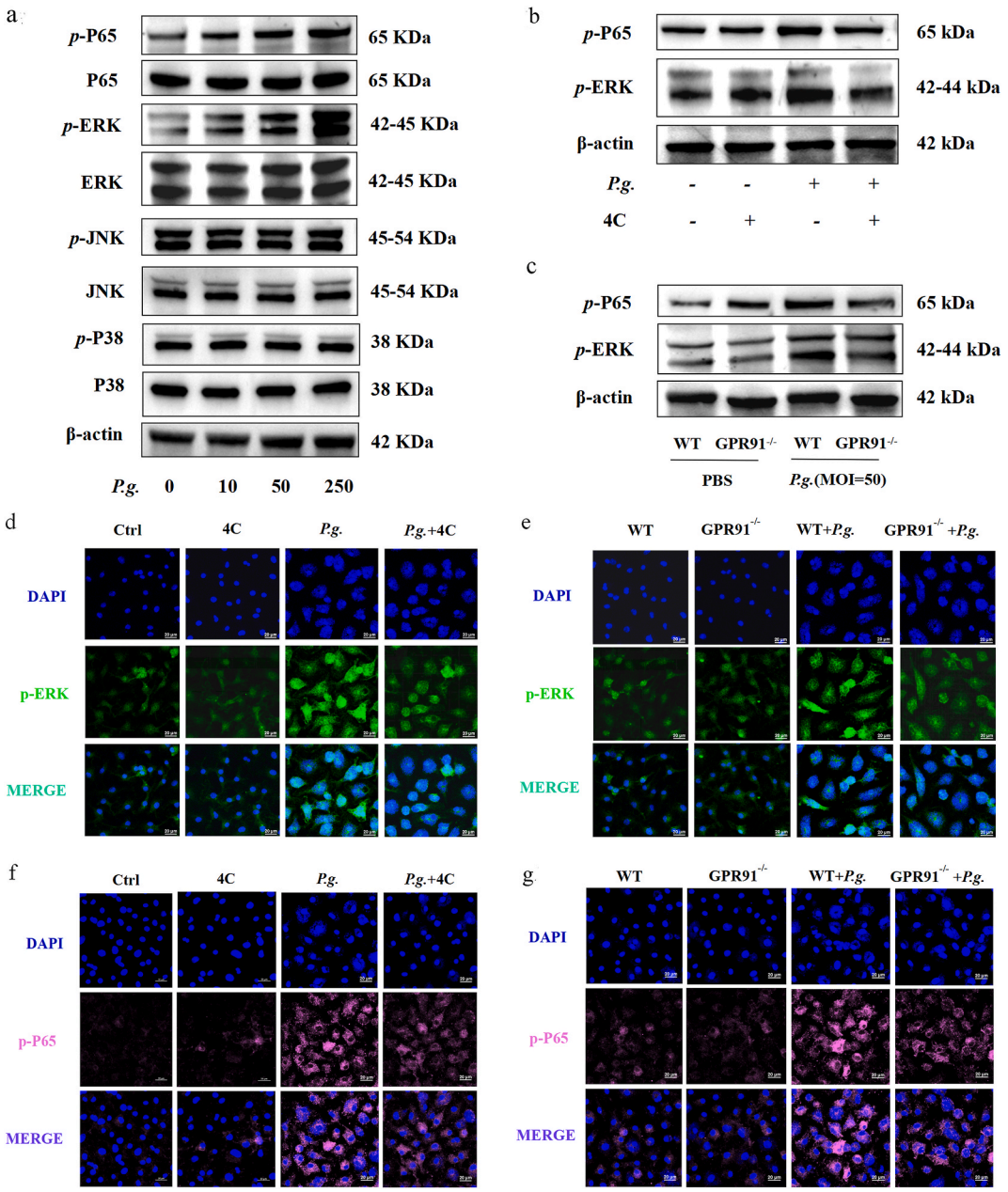

Fig. 5. GPR91-mediated inflammatory responses via the Erk/NFκb signaling pathway in *P. gingivalis*-treated BMDMs. (a) Protein expression was detected by Western Blot after *P. gingivalis* infection (MOI = 10, 50 or 250) at 1 h in BMDMs from WT mice. (b) BMDMs from WT mice were pretreated with 4C (GPR91 antagonist, 5 μM) for 2 h, then infected with *P. gingivalis* (MOI = 50) for 1 h, and the expression of BMDM protein levels was detected by Western Blot. (c) BMDMs from GPR91$^{-/-}$ and WT mice were infected with *P. gingivalis* (MOI = 50) for 1 h, and the protein expression was detected by Western Blot. More details were shown in the Supplemental Information S1. BMDMs from GPR91$^{-/-}$ and WT mice were infected with *P. gingivalis* (MOI = 50) for 12 h (d&e) The expression of *p*-Erk was detected by confocal imaging. (f&g) The expression of *p*-P65 was detected by confocal imaging at 12 h. Image is of a representative Western Blot form one independent experiment. Western Blot and immunofluorescence were performed three times independently. The scale bar represents 20 μm.

significantly increased ROS expression, while GPR91 knockout reduced the stress response(Fig. 4a&b). Excessive ROS in the cytosol can cause membrane polyunsaturated lipids to oxidize, leading to the generation of end products such as malondialdehyde (MDA) [22]. After 24 h of *P. gingivalis* infection, the levels of MDA and superoxide dismutase (SOD) in the BMDMs increased, while GPR91 knockdown decreased the expression of MDA and SOD (Fig. 4c&d).

3.5. GPR91 mediated inflammation in P. gingivalis-treated BMDMs through Erk/NF-κB signaling pathway

Nuclear factor kappa B (NF-κB) is present in nearly all animal cell types and plays a key role in regulating the immune response to infection [23]. The mitogen-activated protein kinase (MAPK) signaling pathway (JNK, p38, Erk) is crucial in the regulation of cellular physiological activities, including inflammatory responses, cellular stress response, cell proliferation, and cellular metabolism. In this study, *P. gingivalis* infection induced elevated extracellular signal-regulated kinase (Erk) and P65 phosphorylation levels, an effect dependent on the *P. gingivalis* MOI concentration (Fig. 5a and Supplemental Information S1). However, *P. gingivalis* infection did not activate the JNK and p38 pathways (Fig. 5a and Supplemental Information S1), suggesting the impact of *P. gingivalis* treatment on MAPK pathway activation is selective.

Subsequently, we treated BMDMs from WT mice with 4C (a GPR91 antagonist, 5 μM) for 2 h prior to *P. gingivalis* infection (MOI = 50). Reductions in the protein expression of *p*-Erk/*p*-P65 were observed in the *P. gingivalis*-infected BMDMs (Fig. 5b and Supplemental Information S1). In addition, *p*-Erk/*p*-P65 levels also decreased in *P. gingivalis*-treated the BMDMs of GPR91$^{-/-}$ mice (Fig. 5c and Supplemental Information S1). Moreover, immunofluorescence analysis confirmed that the expression of *p*-Erk/*p*-P65 in *P. gingivalis*-treated BMDMs was attenuated following either 4C pretreatment or GPR91 knockout (Fig. 5d–g). These findings suggest that GPR91 activation promotes inflammatory responses to *P. gingivalis* in BMDMs via the Erk/NF-κB pathway.

4. Discussion

Metabolic processes at the cellular level are essential for defense against bacterial infection. The rapidly developing field of immunometabolism has provided new insights into the critical roles cellular metabolites and intermediates play in intracellular signaling and intercellular communication [8]. Metabolic reprogramming involves a shift from oxidative phosphorylation to glycolysis that is accompanied by a disruption to the tricarboxylic acid cycle and the accumulation of metabolites such as citrates and succinates. GPR91, a membrane receptor, acts as a sensor that detects the extracellular metabolite succinate. Once transported out of the cytosol, succinate can bind to GPR91, triggering a broad spectrum of physiological and pathogenic effects.

GPR91 has been detected in hepatic stellate cells [24], kidneys [25], and cardiomyocytes [26], and certain types of cancers, as well as within the immune system itself, with functions that include the promotion and migration of cells and tissue remodeling [27]. However, GPR91 has different roles and functions among different cells, tissues, and pathophysiological contexts. In immune cells, intracellular metabolic reprogramming controls cellular behavior, phenotype, and various activation states in response to external stimuli [28]. To further investigate the pathological effects of GPR91 in periodontitis, *P. gingivalis*-infected mouse BMDMs were used in vitro to simulate the periodontal microenvironment. Our findings indicate that *P. gingivalis* worked in conjunction with GPR91 to enhance the expression of intracellular ROS by activating the Erk/P65 pathway, thereby perpetuating the inflammatory state within the periodontal tissues.

GPR91 has previously been shown to upregulates IL-1β expression in the pathophysiology of rheumatoid arthritis (RA), with its effects dependent on succinate concentration [14]. In obesity, on the other hand, GPR91 expression is reduced, resulting in less inflammation in adipose tissue [12]. Consistent with our previous research [6], *P. gingivalis* infection was found to induce metabolic reprogramming in periodontal ligament fibroblasts, leading from oxidative phosphorylation to glycolysis and increasing intracellular succinate. The gingival tissues dynamically alter its metabolism to adapt to the changes of biofilms in the gingival crevicular sulcus. GPR91 expression was detected in human and mouse healthy gingival tissues [29]. As shown in our results (Fig. 1), GPR91 can be found in gingival fibroblasts, oral epithelial cells, and macrophages, and the expression level is higher in inflammatory gingival tissues. However, further macrophages-specific staining of CD11b and F4/80 is needed to confirm the GPR91 expression in macrophages.

The succinate-GPR91 signaling pathway plays a role in immunity and inflammation through the participation of both dendritic cells (DCs) and macrophages [9]. Macrophages, as integral components of the host defense system, are critical during the initial stage of periodontitis for limiting inflammation and repairing tissue [30]. *P. gingivalis*, a red-complex pathogen, has been linked to chronic periodontitis and likely contributes to its progression [31].

In our attempt to further elucidate the role of GPR91 in periodontal inflammation, we investigated the inflammatory response of BMDMs infected by *P. gingivalis.* GPR91 activation has previously shown to increase the expression of proinflammatory cytokines (IL-1β, IL-6 and TNF-α) in M1 macrophages [32], a finding further supported by our study (Figs. 2 and 3). Furthermore, pretreatment with the GPR91-specific inhibitor 4C or GPR91 knockout effectively mitigated *P.* gingivalis-induced inflammation in BMDMs (Figs. 2 and 3). Both GPR91-deficiency and GPR91 antagonist inhibited the release of IL-1β in mice, consistent with a previous mouse model of RA [14]. Interestingly, the results showed that pharmacological inhibition using 4C was more effective in the suppression of TNF-α mRNA expression than GPR91 knockout (Figs. 2 and 3). The pronounced inhibition of TNF-α mRNA by 4C may be GPR91-dependent and independent, and further research is needed to address mechanisms independent of GPR91.

Reactive oxygen species (ROS) are key signaling molecules impacting the progression of inflammatory diseases and are generated by cells involved in the host defense response [33]. Excessive ROS production has been implicated in cellular and tissue damage and the contribute to chronic inflammation underlying multiple neurodegenerative [34], cardiovascular [35], and metabolic diseases [36]. Endothelial cells (EC) rely on ROS production to drive hypoxia-inducible factor 1α (HIF1α) expression and promote glycolysis in

response to hypoxia [37]. ROS production is also associated with an increase in proinflammatory cytokines, such as IL-1β, IL-6, and TNF-α, which are responsible for connective tissue destruction and bone resorption in periodontal tissues [38]. In the 24 h following bacterial infection, ROS increases significantly, acting as a signal that triggers the production of proinflammatory cytokines. Under such conditions, ROS concentration levels remain high to maintain the cells' inflammatory state (Fig. 2d and e). However, after inhibition of GPR91 with 4C, *P. gingivalis*-induced ROS accumulation was significantly reduced, although it had not returned to the baseline levels (Fig. 2d and e). This finding suggests that ROS may contribute to the maintenance of the inflammatory state via GPR91.

Among several ROS-producing systems, the inflammatory enzymes nicotinamide adenine dinucleotide phosphate (NADPH) oxidase and inducible nitric oxide (iNOS) are thought to play major roles [39]. iNOS is not always present in cells but can be induced or stimulated under specific conditions [40]. The large amounts of NO produced by iNOS help to defend against invading pathogens and are therefore essential for the inflammatory response and innate immune system [41]. However, excessive NO concentration, which may be cause by the overexpression or dysregulation of iNOS can lead to toxic effects [40]. Similarly, we found that in macrophages having undergoneGPR91 knockout, *P. gingivalis* treatment for 24 h significantly inhibited iNOS, IL-1β, IL-6, and TNF-α expression and decreased the amount of NO that was subsequently released (Fig. 3). This suggests that GPR91 knockout can limit the accumulation of NO and the production of iNOS caused by *P. gingivalis*.

To investigate the molecular processes underlying the effects of GPR91 in the activation of inflammatory signaling pathways induced by *P. gingivalis.* we examined mitogen-activated protein kinases (MAPKs) and its downstream targets. The MAPK pathways are activated by diverse extracellular and intracellular stimuli including peptide growth factors, cytokines, hormones, and various cellular stressors such as oxidative stress and endoplasmic reticulum stress [42]. In addition, NF-κB has been shown to regulate metabolic reprogramming through the upregulation of mitochondrial respiration [43], while GPR91 activation can induce the phosphorylation of Akt in platelets [44]and Erk in kidney cells [25]. In our study, we observed that *P. gingivalis* activated Erk and NF-κB pathways in macrophages, and when GPR91 was inhibited or knocked out, the levels of Erk 1/2 and NF-κB were reduced (Fig. 5). Similarly, Mills EL et al. [43] found that SUNCR1 was involved in the activation of inflammatory pathways NF-κB and Erk pathways in intestinal epithelial cells. Based on these findings, we posit that GPR91 regulates *P. gingivalis*-induced inflammatory processes through Erk/NF-κB, as evidenced by reduced phosphorylation of this transcription factor in GPR91 knockout cells.

Although our study has provided new insights into the metabolic pathogenesis of periodontitis, some limitations must be acknowledged. Firstly, *P. gingivalis* is recognized as a key pathogen in periodontitis, but the periodontal inflammatory microenvironment involves a complex interplay of pathogenic bacteria. This study only explored the inflammatory changes of BMDMs infected by *P. gingivalis*, which may not fully capture the broader inflammatory response that occurs during periodontitis. In addition, cell death may be one possible explanation for cytokine reduction since minimal cell death was observed at an MOI of 50 in BMDMs infected with *P. gingivalis*, and the data was shown in the new Fig. 2. Although the present study was focused on the inflammatory responses rather than cell death, further studies are needed to explore the role of various types of cell death, such as pyroptosis, necroptosis and ferroptosis. Lastly, to better understand the role of GPR91 in the periodontal inflammatory microenvironment, the establishment of an animal model would provide deeper insights.

5. Conclusion

The present study demonstrated that *P. gingivalis* can induce GPR91 activation, promote ROS generation, and enhance the periodontal inflammatory response. These results suggest that GPR91 may play a role in the pathogenesis of periodontitis by promoting inflammation. Moreover, pharmaceutical inhibition of GPR91 emerges as a potential strategy to regulate periodontal inflammation and mitigate alveolar bone resorption.

Ethics approval and consent to participate

All human experiments are conducted in accordance with the relevant guidelines and regulations. The protocol for collecting normal and diseased gingival samples was approved by the Medical Ethics Committee of Nanjing Stomatological Hospital, Medical School of Nanjing University, and the ethics approval number was 2018NL-007 (KS). The study was approved by approved by the Medical Ethics Committee of Nanjing Stomatological Hospital, Medical School of Nanjing University. Written informed consent was obtained from all subjects and/or their legal guardians.

Data sharing and data accessibility

All data supporting the findings of this study are available from the corresponding author upon reasonable request.

Funding

This study was supported by grants from the National Natural Science Foundation of China (No. 82371007), and Postgraduate Research & Practice Innovation Program of Jiangsu Province (KYCX23_0196).

CRediT authorship contribution statement

Wenqi Su: Writing – review & editing, Writing – original draft, Funding acquisition, Data curation, Conceptualization. **Yujia**

Wang: Writing – original draft, Methodology, Data curation. **Cancan Zu:** Writing – original draft, Data curation. **Lang Lei:** Writing – review & editing, Funding acquisition, Conceptualization. **Houxuan Li:** Writing – review & editing, Conceptualization.

Declaration of competing interest

The authors declare that they have no known competing financial interests or personal relationships that could have appeared to influence the work reported in this paper.

Acknowledgements

We thank Dr. Sheng Chen and Dr. Yan Yang for their excellent technical assistance for immunohistochemistry.

Appendix A. Supplementary data

Supplementary data to this article can be found online at https://doi.org/10.1016/j.heliyon.2024.e34509.

References

[1] J. Mysak, S. Podzimek, P. Sommerova, et al., Porphyromonas gingivalis: major periodontopathic pathogen overview, J Immunol Res 2014 (2014) 476068.
[2] L. Wang, W. Pu, C. Wang, L. Lei, H. Li, Microtubule affinity regulating kinase 4 promoted activation of the NLRP3 inflammasome-mediated pyroptosis in periodontitis, J. Oral Microbiol. 14 (1) (2022) 2015130.
[3] R.D. Pathirana, N.M. O'Brien-Simpson, E.C. Reynolds, Host immune responses to Porphyromonas gingivalis antigens, Periodontol 52 (1) (2000. 2010) 218–237.
[4] E.L. Mills, B. Kelly, A. Logan, et al., Succinate dehydrogenase Supports metabolic Repurposing of mitochondria to drive inflammatory macrophages, Cell 167 (2) (2016) 457–470.e13.
[5] S. Joshi, G. Immanuel, S. Arulrhaj, M. Tiwaskar, A. Vora, S. Samavedam, Roadmap for the Management of Acute Undifferentiated Febrile Illness: an Expert discussion and review of available guidelines, J Assoc Physicians India 69 (9) (2021) 11–12.
[6] W. Su, J. Shi, Y. Zhao, F. Yan, L. Lei, H. Li, Porphyromonas gingivalis triggers inflammatory responses in periodontal ligament cells by succinate-succinate dehydrogenase-HIF-1α axis, Biochem. Biophys. Res. Commun. 522 (1) (2020) 184–190.
[7] M. Trauelsen, E. Rexen Ulven, S.A. Hjorth, et al., Receptor structure-based discovery of non-metabolite agonists for the succinate receptor GPR91, Mol Metab 6 (12) (2017) 1585–1596.
[8] G. Krzak, C.M. Willis, J.A. Smith, S. Pluchino, L. Peruzzotti-Jametti, Succinate receptor 1: an emerging regulator of Myeloid cell function in inflammation, Trends Immunol. 42 (1) (2021) 45–58.
[9] X. Li, L. Xie, X. Qu, et al., GPR91, a critical signaling mechanism in modulating pathophysiologic processes in chronic illnesses, FASEB J. 34 (10) (2020) 13091–13105.
[10] T. Rubic, G. Lametschwandtner, S. Jost, et al., Triggering the succinate receptor GPR91 on dendritic cells enhances immunity, Nat. Immunol. 9 (11) (2008) 1261–1269.
[11] A.L. Saraiva, F.P. Veras, R.S. Peres, et al., Succinate receptor deficiency attenuates arthritis by reducing dendritic cell traffic and expansion of Th17 cells in the lymph nodes, FASEB J. (2018) fj201800285.
[12] N. Keiran, V. Ceperuelo-Mallafré, E. Calvo, et al., SUCNR1 controls an anti-inflammatory program in macrophages to regulate the metabolic response to obesity, Nat. Immunol. 20 (5) (2019) 581–592.
[13] C.J. Aguiar, J.A. Rocha-Franco, P.A. Sousa, et al., Succinate causes pathological cardiomyocyte hypertrophy through GPR91 activation, Cell Commun. Signal. 12 (2014) 78.
[14] A. Littlewood-Evans, S. Sarret, V. Apfel, et al., GPR91 senses extracellular succinate released from inflammatory macrophages and exacerbates rheumatoid arthritis, J. Exp. Med. 213 (9) (2016) 1655–1662.
[15] I. Toma, J.J. Kang, A. Sipos, et al., Succinate receptor GPR91 provides a direct link between high glucose levels and renin release in murine and rabbit kidney, J. Clin. Invest. 118 (7) (2008) 2526–2534.
[16] J. Shi, J. Li, W. Su, S. Zhao, H. Li, L. Lei, Loss of periodontal ligament fibroblasts by RIPK3-MLKL-mediated necroptosis in the progress of chronic periodontitis, Sci. Rep. 9 (1) (2019) 2902.
[17] Y. Yu, L. Jiang, J. Li, L. Lei, H. Li, Hexokinase 2-mediated glycolysis promotes receptor activator of NF-κB ligand expression in Porphyromonas gingivalis lipopolysaccharide-treated osteoblasts, J. Periodontol. 93 (7) (2022) 1036–1047.
[18] L. Jiang, J. Li, K. Ji, L. Lei, H. Li, MAT2A inhibition suppresses inflammation in Porphyromonas gingivalis-infected human gingival fibroblasts, J. Oral Microbiol. 16 (1) (2024) 2292375.
[19] M. Lechner, P. Lirk, J. Rieder, Inducible nitric oxide synthase (iNOS) in tumor biology: the two sides of the same coin, Semin. Cancer Biol. 15 (4) (2005) 277–289.
[20] D. Simpson, P.L. Oliver, ROS generation in Microglia: Understanding oxidative stress and inflammation in neurodegenerative disease, Antioxidants 9 (8) (2020) 743.
[21] Y.T. Deng, K.J. Wu, M.Y. Kuo, Phenytoin induces connective tissue growth factor (CTGF/CCN2) production through NADPH oxidase 4-mediated latent TGFβ1 activation in human gingiva fibroblasts: suppression by curcumin, J. Periodontal. Res. 57 (6) (2022) 1219–1226.
[22] Y. Zhao, J. Li, W. Guo, H. Li, L. Lei, Periodontitis-level butyrate-induced ferroptosis in periodontal ligament fibroblasts by activation of ferritinophagy, Cell Death Discov 6 (1) (2020) 119.
[23] Y. Zheng, Y. Li, X. Ran, et al., Mettl14 mediates the inflammatory response of macrophages in atherosclerosis through the NF-κB/IL-6 signaling pathway, Cell. Mol. Life Sci. 79 (6) (2022) 311.
[24] P.R. Correa, E.A. Kruglov, M. Thompson, M.F. Leite, J.A. Dranoff, M.H. Nathanson, Succinate is a paracrine signal for liver damage, J. Hepatol. 47 (2) (2007) 262–269.
[25] J.H. Robben, R.A. Fenton, S.L. Vargas, et al., Localization of the succinate receptor in the distal nephron and its signaling in polarized MDCK cells, Kidney Int. 76 (12) (2009) 1258–1267.
[26] C.J. Aguiar, V.L. Andrade, E.R. Gomes, et al., Succinate modulates Ca(2+) transient and cardiomyocyte viability through PKA-dependent pathway, Cell Calcium 47 (1) (2010) 37–46.
[27] J.Y. Wu, T.W. Huang, Y.T. Hsieh, et al., Cancer-derived succinate promotes macrophage polarization and cancer Metastasis via succinate receptor, Mol Cell 77 (2) (2020) 213–227.e5.

[28] A.K. Jha, S.C. Huang, A. Sergushichev, et al., Network integration of parallel metabolic and transcriptional data reveals metabolic modules that regulate macrophage polarization, Immunity 42 (3) (2015) 419–430.
[29] Y. Guo, F. Xu, S.C. Thomas, et al., Targeting the succinate receptor effectively inhibits periodontitis, Cell Rep. 40 (12) (2022) 111389.
[30] D. Cui, J. Lyu, H. Li, et al., Human β-defensin 3 inhibits periodontitis development by suppressing inflammatory responses in macrophages, Mol. Immunol. 91 (2017) 65–74.
[31] S.C. Holt, J.L. Ebersole, Porphyromonas gingivalis, Treponema denticola, and Tannerella forsythia: the "red complex", a prototype polybacterial pathogenic consortium in periodontitis, Periodontol 38 (2000. 2005) 72–122.
[32] D.C. Macias-Ceja, D. Ortiz-Masiá, P. Salvador, et al., Succinate receptor mediates intestinal inflammation and fibrosis, Mucosal Immunol. 12 (1) (2019) 178–187.
[33] M. Mittal, M.R. Siddiqui, K. Tran, S.P. Reddy, A.B. Malik, Reactive oxygen species in inflammation and tissue injury, Antioxid Redox Signal 20 (7) (2014) 1126–1167.
[34] K.G. Manton, S. Volovik, A. Kulminski, ROS effects on neurodegeneration in Alzheimer's disease and related disorders: on environmental stresses of ionizing radiation, Curr. Alzheimer Res. 1 (4) (2004) 277–293.
[35] A.J. Serra, J.R. Pinto, M.D. Prokić, G. Arsa, A. Vasconsuelo, Oxidative stress in Muscle diseases: Current and Future Therapy 2019, Oxid. Med. Cell. Longev. 2020 (2020) 6030417.
[36] S. Yang, G. Lian, ROS and diseases: role in metabolism and energy supply, Mol. Cell. Biochem. 467 (1–2) (2020) 1–12.
[37] J.Y. Paik, K.H. Jung, J.H. Lee, J.W. Park, K.H. Lee, Reactive oxygen species-driven HIF1α triggers accelerated glycolysis in endothelial cells exposed to low oxygen tension, Nucl. Med. Biol. 45 (2017) 8–14.
[38] F. Sczepanik, M.L. Grossi, M. Casati, et al., Periodontitis is an inflammatory disease of oxidative stress: we should treat it that way, Periodontol 84 (1) (2000. 2020) 45–68.
[39] S. Koppula, H. Kumar, I.S. Kim, D.K. Choi, Reactive oxygen species and inhibitors of inflammatory enzymes, NADPH oxidase, and iNOS in experimental models of Parkinson's disease, Mediators Inflamm 2012 (2012) 823902.
[40] J.N. Sharma, A. Al-Omran, S.S. Parvathy, Role of nitric oxide in inflammatory diseases, Inflammopharmacology 15 (6) (2007) 252–259.
[41] M.A. Cinelli, H.T. Do, G.P. Miley, R.B. Silverman, Inducible nitric oxide synthase: regulation, structure, and inhibition, Med. Res. Rev. 40 (1) (2020) 158–189.
[42] E.K. Kim, E.J. Choi, Pathological roles of MAPK signaling pathways in human diseases, Biochim. Biophys. Acta 1802 (4) (2010) 396–405.
[43] C. Mauro, S.C. Leow, E. Anso, et al., NF-κB controls energy homeostasis and metabolic adaptation by upregulating mitochondrial respiration, Nat. Cell Biol. 13 (10) (2011) 1272–1279.
[44] C. Högberg, O. Gidlöf, C. Tan, et al., Succinate independently stimulates full platelet activation via cAMP and phosphoinositide 3-kinase-β signaling, J Thromb Haemost 9 (2) (2011) 361–372.